2014 International Joint Conference on Neural Networks (IJCNN)
July 6-11, 2014, Beijing, China

Identification of Meat Spoilage by FTIR Spectroscopy and Neural Networks

Vassilis S. Kodogiannis, Ilias Petrounias, and Eva Kontogianni

***Abstract*—Freshness and safety of muscle foods are generally considered as the most important parameters for the food industry. To address the rapid determination of meat spoilage, Fourier transform infrared (FTIR) spectroscopy technique, with the help of advanced learning-based methods, was attempted in this work. FTIR spectra were obtained from the surface of beef samples during aerobic storage at various temperatures, while a microbiological analysis had identified the population of Total viable counts. A fuzzy principal component algorithm has been also developed to reduce the dimensionality of the spectral data. The results confirmed the superiority of the adopted scheme compared to the partial least squares technique, currently used in food microbiology.**

I. Introduction

THE resolution of the Uruguay Round of the General Agreement on Tariffs and Trade (GATT) in 1995, recognized public health risk as the only basis for restrictions of international trade in food. Beef is one of the commercially viable and widely consumed muscle foods throughout the world. Although it is a good food source for proteins and other essential nutrients, it is also an ideal substrate for the growth of both spoilage and pathogenic microorganisms. The current practice to assure the safety of meat still relies on regulatory inspection and sampling regimes. This approach, however, seems inadequate because it cannot sufficiently guarantee consumer protection, since 100% inspection and sampling is technically, financially and logistically impossible.

Meat industry however needs rapid analytical methods for quantification of these indicators in order to determine suitable processing procedures for their raw material and to predict the remaining shelf life of their products [1]. During previous years, relevant analysis and screening methods had been carried out on meat utilizing high-performance liquid chromatography (HPLC) [2], gas chromatography-mass spectrometry [3] and ion mobility spectrometry [4]. The majority of these methods are however invasive, meaning that either a sample has to be taken or that they are difficult to be implemented on-line. Thus, the introduction of accurate and non-destructive sensing technologies to detect the spoilage bacteria as well as pathogenic bacteria with a high degree of dependency in food products is highly desirable. Various rapid, non-invasive methods based on analytical instrumental techniques, such as Fourier transform infrared spectroscopy (FTIR) [5], Raman spectroscopy [6], and electronic nose technology [7] have been researched for their potential as reliable "meat quality" sensors.

Over the last few years, FTIR has been considered as a very important tool in food analysis including authenticity and adulteration. Nutrient determination is time consuming and not appropriate for routine application in the food industries. FTIR was able to determine omega-6 and omega-3 fatty acids in pork adipose tissue [8]. It has been used to investigate the influence of heating rates and different heating temperatures on protein denaturation in beef [9], as well as to study the influence of ageing and salting on uncooked and cooked pork [10].

The application of chemometric techniques to associate FTIR spectral data with meat spoilage is not new and it has been tackled in the past [11]. However, emphasis was considered only with the detection of bacterial spoilage, in terms of microbiological analysis, whereas no attempt was made to associate spectral data with quality classes defined by sensory assessment of the samples. FTIR spectral data collected directly from the surface of meat were verified that they could be used as biochemical interpretable "signatures", in an attempt to obtain information on early detection of microbial spoilage of chicken breast and rump steaks [12]. A series of partial least squares (PLS) models and simple multilayer neural networks (MLP) have been investigated, to correlate spectral data from FTIR spectroscopy analysis with beef spoilage and its associated total viable bacteria counts-TVC [13].

The main objective of this paper is to associate FTIR spectral data with beef spoilage during aerobic storage at various temperatures (0, 5, 10, 15, 20 °C) utilizing an advanced learning-based decision support system. Information related to FTIR spectra, as well as the correlated microbiological analysis (*i.e.* total viable counts - TVC) from beef fillets, was made accessible from Agricultural University of Athens in the framework of the Symbiosis-EU European research project. Due to the nature of FTIR spectral data, it is necessary to consider the use of a dimensionality reduction algorithm to reduce the problem of dimensionality with the minimum information lost. Principal components analysis (PCA) is an unsupervised method that transforms a large number of potentially correlated factors into a small number

V.S. Kodogiannis is with Faculty of Science and Technology, University of Westminster, 115 New Cavendish Street, London W1W 6UW, United Kingdom (phone: +44-7775708976, e-mail: kodogiv@westminster.ac.uk).

I. Petrounias is with the Manchester Business School, University of Manchester, United Kingdom (e-mail: ilias.petrounias@manchester.ac.uk).

E. Kontogianni is with the General Directorate of Development, Regional Unit of Heraklion, Crete, Greece.

978-1-4799-1484-5/14/$31.00 ©2014 IEEE

of orthogonal (uncorrelated) factors, reducing thus the size of the initial dataset and optimizing the feature vector [14]. However, it is well-known that PCA is vulnerable with respect to outliers, missing data, and poor linear correlation between variables due to poorly distributed variables [15]. As a result, it is important to make PCA more robust. In this research study, an improvement of PCA is proposed by the fuzzification of the matrix data, in order to reduce the influence of the outliers. In the current study, a novel neural network scheme based on the Extended Normalized Radial Basis Function network (ENRBF) has been developed to classify beef samples to one of three quality classes (*i.e.* fresh, semi-fresh, and spoiled) based on the biochemical profile provided by the FTIR spectra dataset. The same model simultaneously is able to predict the microbial load on meat surface. The Bayesian Ying-Yang (BYY) Expectation Maximization (EM) algorithm has been used together with novel splitting operations to determine network's size and parameter set. Results from ENRBF are compared against models based on partial least squares (PLS). Such comparison is considered as an essential practice, as we have to emphasize the need of induction to the area of food microbiology, advanced learning-based modeling schemes, which may have a significant potential for the rapid and accurate assessment of meat spoilage. Such an accurate assessment prediction could allow a more efficient management of products in the food chain.

I. FTIR Sampling and Analysis

The FTIR experimental case was performed at the Laboratory of Microbiology and Biotechnology of Foods, of the Agricultural University of Athens, Greece. A detailed description of the experimental methodology as well as the related microbiological analysis of the meat samples is described in [16]. Briefly, the samples were prepared by cutting fresh pieces of beef into small portions ($40mm$ wide $\times$ $50mm$ long $\times$ $10mm$ thick) and then portions placed onto Petri dishes and stored at $(0, 5, 10, 15 \text{ and } 20\ ^{\circ}C)$ in high-precision $(\pm 0.5\ ^{0}C)$ incubation chambers for a total period of $350h$, taking into consideration the storage temperature, until spoilage was apparent. For the purposes of FTIR spectral measurements, a thin slice of the aerobic upper surface of the beef fillet was isolated and used for additional analysis. In total, 74 FTIR spectra were produced through the use of a using a ZnSe 45^{o} ATR (Attenuated Total Reflectance) crystal on a Nicolet 6700 FTIR Spectrometer. These spectra were collected over the wave-number range 4000 to 400cm^{-1} , whilst the scans per measurement were 100 with a resolution of 4cm^{-1} , resulting in a total integration time of 2 min [13].

In parallel, microbiological analysis was performed, and resulting growth data from plate counts were log10 transformed and fitted to the primary model of Baranyi & Roberts [17] in order to verify the kinetic parameters of microbial growth (maximum specific growth rate and lag phase duration). The population dynamics of total viable counts (TVC) for beef fillet storage at different temperatures, under aerobic conditions, is illustrated in Fig. 1. Analysis specified that the total microflora ranged from $2.9 - 3.3 \log_{10}$ cfu cm^{-2} at the beginning of storage (fresh samples), to $8.7 - 9.4 \log_{10}$ cfu cm^{-2} for samples characterized as spoiled.

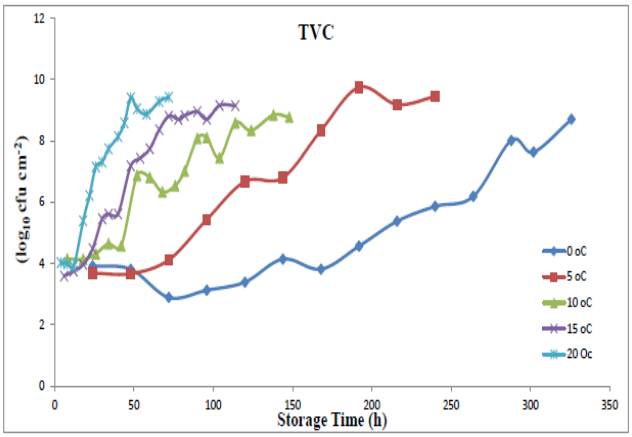

Fig. 1. Growth Curves of TVC at different temperatures for beef samples

This finding is consistent with an indication that the population threshold that depicts the shift of a sample from fresh to semi-fresh and then from semi-fresh to spoiled is temperature dependant. Sensory evaluation of meat samples was performed during storage, based on the perception of color and smell before and after cooking. Each sensory attribute was assigned to a three-point scale corresponding to: 1=fresh; 2=semi-fresh; and 3= spoiled. In total, 74 meat samples were evaluated by a sensory panel and classified into the selected three groups as fresh (n = 24), semi-fresh (n = 16), and spoiled (n = 34) for the case of TVC [13]. Dataset consisted of the TVC values as well as the sensory categorization was utilized for the development of the proposed prediction and classification intelligent-based model.

II. Extended Normalised Radial Basis Function Networks

An alternative formulation of the Radial Basis Function (RBF) network is used in this study. The Extended Normalized RBF (ENRBF) network replaces the linear combiner of the RBF with a series of local linear models [18] as shown in Fig. 2. We propose a supervised training method for this scheme that is fully supervised as it incorporates the Bayesian Ying-Yang (BYY) [19] method for parameter updating and uses a heuristic to determine the starting parameters of the network [20].

The BYY Expectation Maximization (EM) method treats the problem of optimization as one of maximizing the entropy between the original non-parametric data distribution based on Kernel estimates or user specified values and the parametric distributions represented by the network. This is achieved through the derivation of a series of EM update equations using a series of entropy functions as the Q function

or log-likelihood function. The ENRBF network can be represented by the following set of equations.

$$E(z \mid x,\Theta) = \frac{\sum_{j=1}^{K}\left(W_j^T x + c_j\right) p\left(x \mid j,\theta_j\right)}{\sum_{j=1}^{K} p\left(x \mid j,\theta_j\right)} \tag{1}$$

where z is the output of the network $z \in Z$, x is an input vector $x \in X$, $\Theta = [W, c, \theta]$ are the network parameters and $\theta = [m, \Sigma]$ are the parameters of the Gaussian activation functions given by.

$$p\left(x \mid j,\theta_j\right) = \exp\left\{-\tfrac{1}{2}\left(x - m_j\right)^T \Sigma_j^{-1}\left(x - m_j\right)\right\} \tag{2}$$

The BYY method attempts to maximize the degree of agreement between the expected value of z from the network and the true value of z from the training data. It is guaranteed to lead to a local optimum and unlike the original EM algorithm for learning the parameters of Gaussian functions this method encourages coordination between the input and output domains [19].

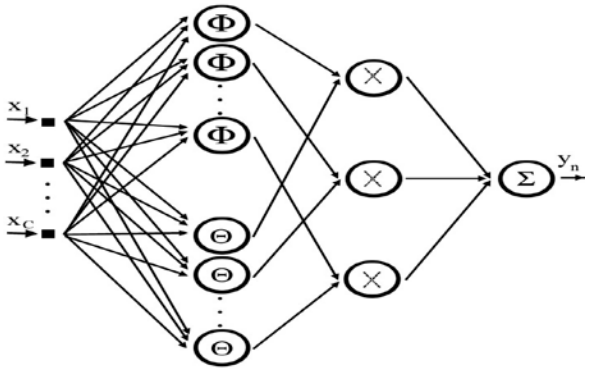

Fig. 2. ENRBF scheme

Like the EM algorithm, this method is very fast in terms of the number of iterations needed for the parameters to converge. It is this speed of convergence that makes the proposed technique feasible. However, as BYY is an EM based technique it is still susceptible to locally maximal values. The Split and Merge EM (SMEM) concept for Gaussian Mixture Models (GMM) proposed initially by Ueda, has been applied to the ENRBF scheme [18]. The original SMEM algorithm is able to move neurons from over populated areas of the problem domain to underrepresented areas by merging the over populated neurons and splitting the under-populated. The use of Eigenvectors to split along the axis of maximum divergence instead of randomly as in original SMEM has been proposed recently [21]. The SMEM algorithm suffers from the fact that before terminating all possible combinations of Split and Merge operations must be examined. Although many options can be discounted, the training still increases exponentially with network size and again suffers from the problems inherent with k-means and basic EM. A splitting technique that overcomes these problems has been proposed by one of the authors [22].

A. The Bayesian Ying-Yang training

This is a supervised training method for ENRBF models it was originally proposed by Ueda [23] and has been used in other studies by the authors [22]. For a network of a given number of normalised Gaussian neurons and their corresponding linear models the following update equations are performed until convergence for each neuron $j<=K$ [19].

$$h\left(j \mid x_i\right) = \frac{P\left(x_i \mid j,\theta_j^{old}\right) P\left(z_i \mid r_j^{old},\Gamma_j^{old}\right)}{\sum_{j=1}^{K} P\left(x_i \mid j,\theta_j^{old}\right) P\left(z_i \mid r_j^{old},\Gamma_j^{old}\right)} \tag{3}$$

$$P\left(z_i \middle| r_j^{old},\Gamma_j^{old}\right) = \exp\left(-\frac{1}{2} D_j^i\right) \tag{4}$$

$$D_j^i = \left(z_i - W_j^{old} - c_j^{old}\right)\left(\Gamma_j^{old}\right)^{-1}\left(z_i - W_j^{old} - c_j^{old}\right)$$

$$m_j^{new} = \frac{\sum_i^N h\left(j \mid x_i\right) x_i}{\sum_i^N h\left(j \mid x_i\right)} \tag{5}$$

$$\Sigma_j^{new} = \frac{\sum_i^N h\left(j \mid x_i\right)\left(x - m_j\right)\left(x - m_j\right)^T}{\sum_i^N h\left(j \mid x_i\right)} \tag{6}$$

$$Ez_j = \frac{\sum_{i=1}^N h\left(j \middle| x_i\right) z_i}{\sum_{i=1}^N h\left(j \middle| x_i\right)} \tag{7}$$

$$R_{xz} = \frac{\sum_{i=1}^N h\left(j \middle| x_i\right)\left[x_i - m_j^{new}\right]\left[z_i - Ez_j\right]^{\mathrm{T}}}{\sum_{i=1}^N h\left(j \middle| x_i\right)} \tag{8}$$

$$W_j^{new} = \left[\Sigma_j^{new}\right]^{-1} R_{xz} \tag{9}$$

$$c_j^{new} = Ez_j - \left(W_j^{new}\right)^{\mathrm{T}} m_j^{new} \tag{10}$$

$$\Gamma_j^{new} = \frac{\sum_{i=1}^N h\left(j \middle| x_i\right) B_j^i}{\sum_{i=1}^N h\left(j \middle| x_i\right)} \tag{11}$$

$$B_j^i = \left[z_i - \left(W_j^{new}\right)^{\mathrm{T}} x_i - c_j^{new}\right]\left[z_i - \left(W_j^{new}\right)^{\mathrm{T}} x_i - c_j^{new}\right]^{\mathrm{T}}$$

III. Modified ENRBF with Split operation

The BYY training method described above is guaranteed to lead to a locally optimum set of network parameters, in terms of the Q function, from a given initial parameter set [19]. This means that the accuracy of the network is dependent on the initial parameter guesses entered by the system designer often these are random values. In this paper, an alternative methodology is proposed by starting with a single Gaussian neuron and then gradually increasing the size of the network until an optimum network size is selected by a model order selection criteria [21]. After the BYY EM algorithm has converged for each network the neuron with the worst fit of the data it covers is selected and then the following operations are performed increasing the size of the network before re-training and testing against the model order selection criteria. The split operation is performed in such a way as the

location of the data in both the input and output domains is taken into account when calculating the new starting parameters for the BYY EM training algorithm. The split operation attempts to first establish a greater accuracy in the output domain *Z* before attempting to gain a more intricate model of the input domain.

A. Selecting the neuron to split

The selection of the neuron to be split is done by assuming that the output of the network is actually a probability of the power plant needing to perform at full capacity. As a result the local Kullback-Leiber divergence can be used to calculate the difference between the output of the neuron given by the local linear model and the actual desired output *Z*.

$$E\left(z_i \middle| x_i, \Theta_j\right) = \frac{\left(W_j^T x_i + c_j\right) P\left(x_i \middle| j, \theta_j\right)}{\sum_{j=1}^{K} P\left(x_i \middle| j, \theta_j\right)} \tag{12}$$

$$J_{split}(k) = -\sum_{i=1}^{N}\sum_{j=1}^{L} E\left(z_{i,l} \middle| x_{i,j}, \Theta_k\right) \ln\left\{\frac{E\left(z_{i,j} \middle| x_{i,j}, \Theta_k\right)}{z_{i,j}}\right\} \tag{13}$$

$$ind = \arg\max_k \left\{J_{split}\right\}, k = \{1,...,K\}$$

The maximum value of J_{split} corresponds to the neuron with the worst fit of the data covered by its Gaussian activation function.

B. The split operation

The first set of operations attempts to discover a desired output for each of the new neurons. This is done by creating two new expected mean output values *Ez* along the main axis of deviation in the output distribution using the Eigenvalues and Eigenvectors of the distribution.

$$\left|\Gamma_{ind} - \lambda I\right| = 0, \lambda = \{\lambda_1,...,\lambda_C\} \tag{14}$$

$$\left(\Gamma_{ind} - \lambda_i I\right) v_i = 0, V = \{v_1,...,v_C\} \tag{15}$$

$$Ez_{ind} = P\left(z \middle| ind\right) + V\lambda' \tag{16}$$

$$Ez_{K+1} = P\left(z \middle| ind\right) - V\lambda' \tag{17}$$

It is then possible to compute new output deviations based on the distance of each mean from the training samples and the relevance of that training sample to the original neuron that is being split. Here, $j = \{ind, K+1\}$

$$\Gamma_{ind}^{new} = \frac{\sum_{i=1}^{N} d_j(x_i) h\left(ind \mid x_i\right)\left(z_i - Ez_j\right)\left(z_i - Ez_j\right)^{\mathrm{T}}}{\sum_{i=1}^{N} d_j(x_i) h\left(j \mid x_i\right)} \tag{18}$$

where

$$d_{ind}(x_i) = \begin{cases} 1, if \left|Ez_{ind} - z_i\right| <= \left|Ez_{K+1} - z_i\right| \\ 0, otherwise \end{cases} \tag{19}$$

and

$$d_{K+1}(x_i) = \begin{cases} 1, if \left|Ez_{K+1} - z_i\right| <= \left|Ez_{ind} - z_i\right| \\ 0, otherwise \end{cases} \tag{20}$$

This provides information relating to the locations of each of the two new neurons in the output space. If these are similar or identical then the two neurons are simply attempting to get a better resolution of the input data. In this case the split can be done simply based on the distribution of the input domain. If they are different then a new feature space in the data has been discovered and the split should be performed in order to take into account the distribution in the input domain of those data points that are closest to the new output mean. Taking a Euclidean distance measure between the two output means represents this distinction. The closer the distance is to 1, the more likely the two new neurons represent distinct data areas in the input domain. The closer to 0 the distance is then the higher the likelihood that the split has been performed in order to gain better representation of the input domain within a single area. In this case, then a split is performed along the largest axis of the neuron being split again using the Eigenvalues and Eigenvectors of the Gaussian activation function of the neuron [21].

$$dis = \left|Ez_{ind} - Ez_{K+1}\right| \tag{21}$$

$$\left|\Sigma_{ind} - \lambda I\right| = 0, \ \lambda = \{\lambda_1,...,\lambda_M\} \tag{22}$$

$$\left(\Sigma_{ind} - \lambda_i I\right) v_i = 0, \ V = \{v_1,...,v_C\} \tag{23}$$

$$m\_t_{ind} = m_{ind} + V\lambda' \tag{24}$$

$$m\_t_{K+1} = m_{ind} - V\lambda' \tag{25}$$

With this information it is possible to compute the new parameters of the neurons. Here, $j = \{ind, K+1\}$

$$\begin{aligned} out_j(x_i) &= (dis)\, d_j(x_i) h\left(ind \middle| x_i\right) \\ in_j(x_i) &= (1 - dis)\, d\_i_j(x_i) h\left(ind \middle| x_i\right) \end{aligned} \tag{26}$$

$$m_j^{new} = \frac{\sum_i^N out_j(x_i) x_i + in_j(x_i) x_i}{\sum_i^N out_j(x_i) + in_j(x_i)} \tag{27}$$

$$\Sigma_j^{new} = \frac{\sum_i^N out_j(x_i) G_{i,j} + in_j(x_i) G_{i,j}}{\sum_i^N out_j(x_i) + in_j(x_i)} \tag{28}$$

$$G_{i,j} = \left(x - m_j^{new}\right)\left(x - m_j^{new}\right)^{\mathrm{T}}$$

$$R_j = \frac{\sum_{i=1}^N out_j(x_i) E_{i,j} + in_j(x_i) E_{i,j}}{\sum_{i=1}^N out_j(x_i) + in_j(x_i)} \tag{29}$$

$$E_{i,j} = \left[x_i - m_j^{new}\right]\left[z_i - Ez_j\right]^{\mathrm{T}}$$

$$W_j^{new} = \left[\Sigma_j^{new}\right]^{-1} R_j \tag{30}$$

$$c_j^{new} = Ez_j - \left(W_j^{new}\right)^{\mathrm{T}} m_j^{new} \tag{31}$$

where

$$d\_i_{ind}(x_i) = \begin{cases} 1, if \left|m\_t_{ind} - x_i\right| <= \left|m\_t_{K+1} - x_i\right| \\ 0, otherwise \end{cases}$$

and

$$d\_i_{K+1}(x_i)=\begin{cases}1, if\ |m\_t_{K+1}-x_i|<=|m\_t_{ind}-x_i|\\ 0, otherwise\end{cases} \quad (32)$$

At this point $K=K+1$ and BYY EM training can recommence.

IV. Data Analysis

In this work, FTIR spectral information was utilized to obtain metabolic "signatures" of beef fillet samples during storage in aerobic conditions at five different storage temperatures (0, 5, 10, 15, and 20 °C). Typical FTIR spectral data in the range of $1800-1000\text{cm}^{-1}$ collected from fresh and spoiled beef fillet samples stored at 10 °C for 6 days are shown in Fig. 3.

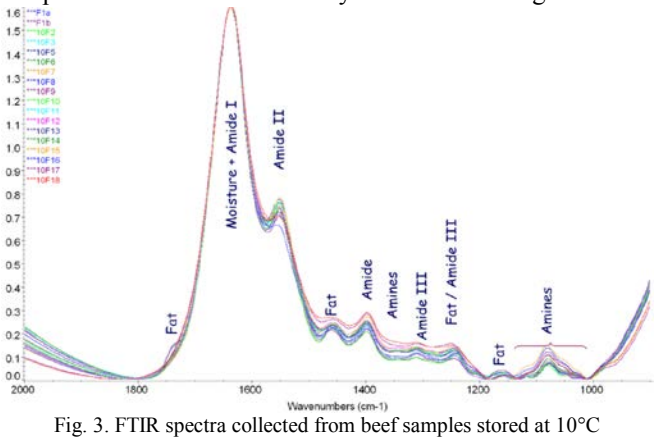

Fig. 3. FTIR spectra collected from beef samples stored at 10°C

Information from these spectra can be extracted in order to acquire metabolic fingerprints of beef fillets during storage at various temperatures. A principal component analysis (PCA) was then performed on this mean-centered spectral data. In this particular experimental case study, although the total variance (100%) of the dataset was explained by 37 principal components (PCs), only the first five PCs were associated with the 97.85% of the total variance, as shown in Table I.

TABLE I
RESULTS FOR PCA AND FPCA SCHEMES

PCs	PCA			FPCA		
	E. value	Prop. %	Cum. prop. %	E. value	Prop. %	Cum. prop. %
1	6.060	47.874	47.874	2.670	57.405	57.405
2	2.528	19.971	67.845	1.845	39.667	97.072
3	1.824	14.409	82.254	0.063	1.354	98.426
4	1.391	10.989	93.243	0.041	0.881	99.307
5	0.583	4.606	97.849	0.019	0.408	99.715

An alternative solution to improve PCA appears to be the fuzzification of the matrix data [24]. One approach toward the fuzzification of the matrix data is to consider the points that are isolated with respect to the first principal component. Fuzzy membership degrees can be introduced according to the distance to the first principal component. As such, fuzzy clustering schemes could be used to determine the first fuzzy principal component and the corresponding fuzzy membership degrees. The algorithm could be considered as an extension of the fuzzy regression algorithm. The fuzzy set in this case may be characterized by a linear support, denoted $L(u,\upsilon)$, where υ is the centre of the class and u, with $\|u\|=1$, is the main direction. This line is named the first principal component for the set, and its direction is given by the unit eigenvector u associated with the largest eigenvalue $\lambda_{\max}$ of the following fuzzy covariance matrix which is a slight generalization for fuzzy sets of the classical covariance matrix

$$C_{ij}=\frac{\sum_{k=1}^{p}A(x^k)^m\left(x_i^k-\overline{x}_i\right)\left(x_j^k-\overline{x}_j\right)}{\sum_{k=1}^{p}A(x^k)^m},\quad i,j=1,\ldots,n \quad (33)$$

The fuzzy objective function is then defined as

$$J(A,L;\alpha)=\sum_{j=1}^{n}\left[A(x^j)\right]^2 d^2(x^j,L)+\sum_{j=1}^{n}\left[\overline{A}(x^j)\right]^2\frac{\alpha}{1-\alpha} \quad (34)$$

where $\{A,\overline{A}\}$ is the fuzzy partition ($\overline{A}$ is the complementary fuzzy set), and α is a real constant from the interval $(0,1)$ which represents the membership degree of the farthest point (the largest outlier) from the first principal component. The support $L(u,\upsilon)$ that minimizes the function $J(\bullet)$ is given by

$$\upsilon=\sum_{j=1}^{n}\left[A(x^j)\right]^m x^j \Big/ \sum_{j=1}^{n}\left[A(x^j)\right]^m \quad (35)$$

Where the fuzzy membership degree $A(x^j)$ is defined as

$$A(x^j)=\frac{\frac{\alpha}{1-\alpha}}{\frac{\alpha}{1-\alpha}+\left(d^2(x^j,L)\right)^{\frac{1}{m-1}}} \quad (36)$$

Since α is an input parameter, a heuristics for determining the best suitable value of it is desirable. The main interest is to find fuzzy membership degrees which contribute to producing a better fitted first principal component along the data set. But, since the eigenvalue associated to a principal component describes the scatter of data along that component, we are also interested in producing a first principal component characterized by an eigenvalue that is as large as possible. Consequently, the optimal solution is that particular value of α which maximizes the eigenvalue associated to the first principal component.

Concerning the FPCA, of the same data set we have to remark that the results obtained are quite different. We can see that, for example, the first principal component explains 57.4% of the total variance and the second one 39.66; a two component model thus accounts for 97.07% of the total

variance (as compared to 67.84% for PCA) and a three components model accounts for 98.42% (as compared to 82.25% for PCA) (Table I). Clearly, the first FPCA-derived components account for significantly more of the variance than the PCA counterparts. Thus, the first three principal components from the FPCA were extracted and utilized as inputs to the various simulation models applied on this particular dataset.

V. Results and Discussions

A machine learning approach based on the proposed ENRBF model has been adopted in order to create a dual model acting as an efficient classifier, in an effort to classify meat samples in three quality classes (fresh, semi-fresh, spoiled) and simultaneously as a predictor.

ENRBF has been implemented through MATLAB and its structure, as shown from Fig. 2, consists of an input layer which in this current research study contains five input nodes (*i.e.* storage temperature, sampling time, and the values of the first three principal components). The output layer consists of two nodes, corresponding to the predicted quality class (fresh, semi-fresh, spoiled) of meat samples and the related microbiological attribute, respectively. The initial FTIR dataset was divided into a training subset with approx. 80% of the data, and a testing subset with the remaining 20% (*i.e.* 14 samples).

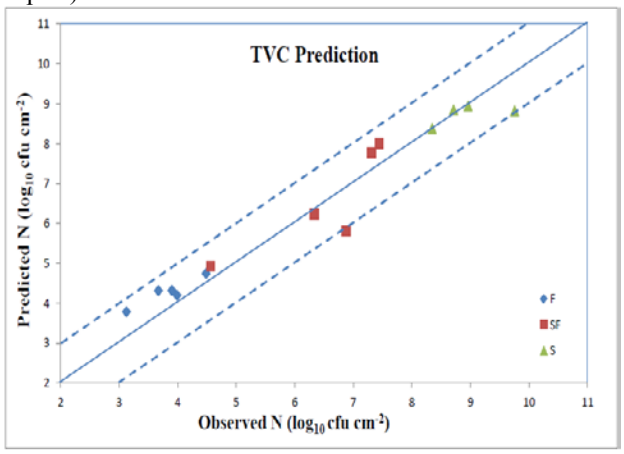

Fig. 4. ENRBF prediction model for TVC

As both output parameters are not independent, in the sense that quality class is related to microbiological counts and vice versa, a model that combines both these measurements have been considered to be desirable. In order to accommodate both classification and modeling tasks in the same model-structure, the classification task has been modified accordingly. Rather than trying to create a distinct classifier, an effort has been made to "model" the classes [25]. Initially, values of 10, 20 and 30, have been used respectively, to associate the three classes with a cluster centre. During the identification process, the output values of $[5.....15]$ were associated to "fresh" class with cluster centre 10, values of $[15.01.....25]$ were associated to "semi-fresh" class with cluster centre 20, and finally values of $[25.01.....35]$ were associated to "spoiled" class with cluster centre 30. The second output node has been assigned to the individual microbiological feature. The classification accuracy of the ENRBF network was determined by the number of correctly classified samples in each sensory class divided by the total number of samples in the class. The performance of the model for the prediction of each microbiological feature for each meat sample was determined by the bias (B_f) and accuracy (A_f) factors, the mean absolute percentage error (MAPE), and finally by the root mean squared error (RMSE) and the standard error of prediction (SEP) [26].

TABLE II
PERFORMANCE OF ENRBF AND PLS MODELS FOR TVC

Statistical index for TVC (testing dataset)	Fresh	Semi-fresh	Spoiled	Overall (ENRBF)	Overall (PLS)	Overall-PLS (leave-1-out)
Mean squared error (MSE)	0.2287	0.3592	0.2214	0.2733	2.452	1.4936
Root mean squared error (RMSE)	0.4783	0.5994	0.4706	0.5227	1.566	1.2221
Mean absolute percentage error (MAPE)	0.1213	0.0777	0.0293	0.0794	0.243	0.1792
Bias factor (B_f)	1.1195	1.0058	0.9798	1.0372	1.064	0.9609
Accuracy factor (A_f)	1.1195	1.0820	1.0309	1.0802	1.2366	1.2121
Correlation coefficient (R^2)- overall				0.9759	0.7213	0.8262
Standard error of prediction (SEP %)	12.4714	9.2144	5.2620	8.3669	25.066	18.5961

In addition to ENRBF model, PLS regression models have been developed for TVCs, utilizing the same training/testing dataset, as well as the same input variables set. PLS models were implemented also in MATLAB, with the aid of PLS Toolbox. The nonlinear iterative partial least squares algorithm (NIPALS) has been chosen as the appropriate learning scheme. A critical aspect in PLS model development was the determination of the optimal number of Latent Variables (LVs). Using too few LVs results in an insufficient model, but using too many variables an unnecessary over-fitting may occurs. A number of 3 LVs was finally selected presenting the highest percentage of accuracy during model development for TVCs.

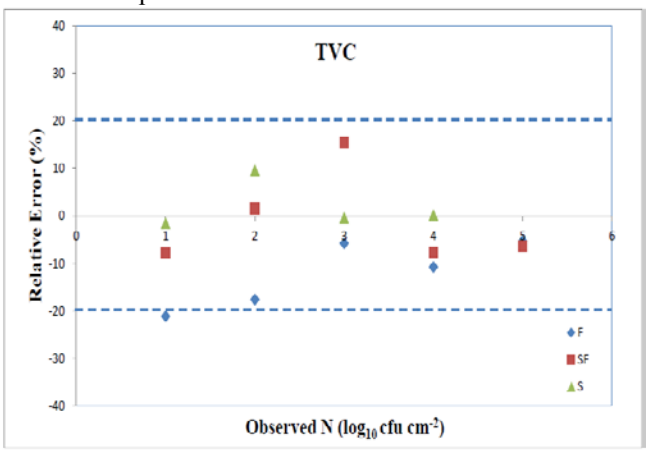

Fig. 5. ENRBF's Residual Error performance

The plot of predicted (via ENRBF) versus observed total viable counts is illustrated in Fig. 4, and shows a very good distribution around the line of equity (y=x), with all the data included within the ±1 log unit area. The performance of the

ENRBF model is also presented in Fig. 5, where the % relative error of prediction is illustrated against the observed microbial population. Based on this plot, data was almost equally distributed above and below 0, with all (expect one) predicted TVC counts included within the ±20% RE zone.

A close inspection in both illustrations, reveal some interesting conclusions. Two samples, as shown from Fig. 4, are in the border line of the ±1 log unit area and they are associated to the semi-fresh "10F7" and the spoiled "5F9" samples. "10F7" corresponds to a beef fillet, stored at 10°C and collected after 52h of storage, while "5F9" was stored at 5°C and collected after 192h of storage.

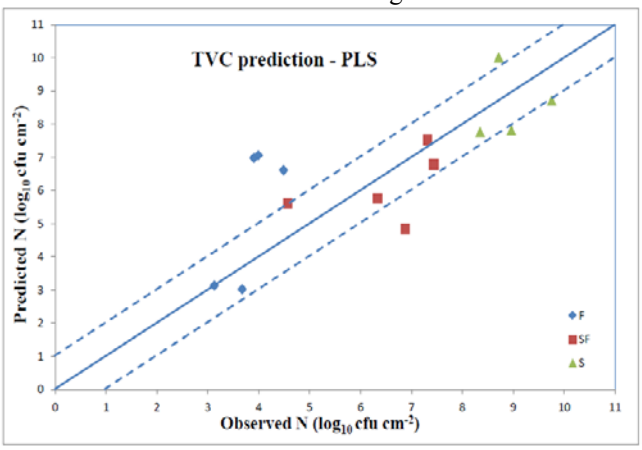

Fig. 6. PLS prediction model for TVC

Two fresh samples (*i.e.* "0F5" and "5F3") are close to the border line at Fig. 4, and the same samples appear to be in the vicinity of the border of the ±20% RE zone at Fig. 5. "0F5" corresponds to a beef fillet, stored at 0°C and collected after 96h of storage, while "5F3" was stored at 5°C and collected after 48h of storage. It seems that all these "suspicious" cases occur at low temperatures. TVC illustrations at Fig. 1, reveals that both 0°C and 5°C curves have an initial flat response, which could justify such "suspicious" behavior. A possible way to overcome this problem could be to broaden the training dataset, especially for low temperatures. The performance of the ENRBF model in predicting TVCs in beef samples in terms of statistical indices is presented in Table II.

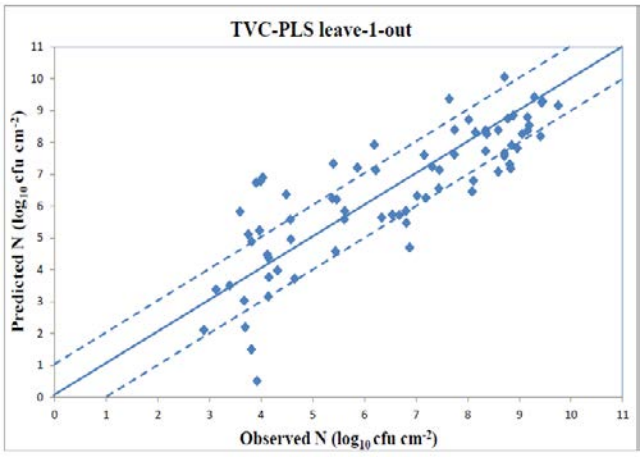

Fig. 7. PLS prediction model for TVC (leave-1-out case)

Two PLS models have been implemented utilizing the same FTIR information. The first model was trained exactly on the same, as in the ENRBF case, dataset, while the second one was trained through a leave-1-out validation method. Their performance for predicting TVCs is shown at Figs. 6 and 7, while the related statistical information is illustrated at Table II.

Results also revealed that the classification accuracy of the ENRBF model was very satisfactory in the characterization of meat samples, indicating the advantage of a "Gaussian-based" approach in tackling complex, nonlinear problems, such as meat spoilage. The classification accuracy obtained from ENRBF, is presented in the form of a confusion matrix in Table III. The model overall achieved a 92.85% correct classification, and 100%, 80% and 100% for fresh, semi-fresh and spoiled meat samples, respectively.

TABLE III
CONFUSION MATRIX FOR ENRBF ACTING AS CLASSIFIER

True class	**Predicted class**			**Row total (n_i)**	**Sensitivity (%)**
	Fresh	Semi-fresh	Spoiled		
Fresh (n = 5)	5	0	0	5	100
Semi-fresh (n = 5)	0	3+1(marginally)	1	5	80
Spoiled (n = 4)	0	0	4	4	100
Column total (n_j)	5	4	5	14	
Specificity (%)	100	100	80		
Overall correct classification (accuracy): 92.85%					

The sensitivities (*i.e.* how good the network is at correctly identifying the positive samples) for fresh and spoiled meat samples reveal a perfect matching. In the case of semi-fresh samples, one sample was marginally classified as semi-fresh, while another one was clearly classified as spoiled. The specificity index (*i.e.* how good the network is at correctly identifying the negative samples) was also high, indicating satisfactory discrimination between these three classes (Table III). It is characteristic that no fresh samples were misclassified as spoiled and vice versa, indicating that the biochemical information provided by FTIR data could discriminate these two classes accurately. Lower percentages were obtained for spoiled samples (ca. 80%) with incorrect classifications in the semi-fresh class. The lower accuracies obtained in the semi-fresh class could be also attributed to the performance of the sensory evaluation process, as the difference between "fresh" and "semi-fresh" class is not very obvious sometimes.

VI. Conclusions

In conclusion, this simulation study demonstrated the effectiveness of the detection approach based on FTIR spectroscopy which in combination with an appropriate machine learning strategy could become an effective tool for monitoring meat spoilage during aerobic storage at various temperatures. The collected spectra could be considered as biochemical "signatures" containing information for the

discrimination of meat samples in quality classes corresponding to different spoilage levels, whereas in the same time could be used to predict satisfactorily the microbial load directly from the sample surface. The current research however revealed two open problems. The use of any machine learning method cannot be considered as panacea to problems that include sensorial devices. It is well known that PLS regression models do have problems in modeling high nonlinear dynamics problems [27]. There is need to explore further the use of advanced intelligent systems, and this paper has attempted for the first time to associate FTIR spectra with such systems. The ENRBF performance although very convincing, discloses however a second open problem, that is the need to have or "create" large training datasets, even with the presence of small amount of real experimental data. Research work is in progress to develop algorithms based on fuzzy logic that will generate "virtual" spectral data from limited experimental spectral meat samples.

ACKNOWLEDGMENT

The FTIR dataset, as well as the TVCs that correspond to the experimental beef samples were supplied by the Agricultural University of Athens, in the framework of the Symbiosis-EU project.

REFERENCES

[1] B. Dissing, O. Papadopoulou, C. Tassou, B. Ersbøll, J. Carstensen, E. Panagou, G-J. Nychas, "Using Multispectral Imaging for Spoilage Detection of Pork Meat", *Food and Bioprocess Technology*, vol. 6, No. 9, pp. 2268-2279, 2013

[2] G. Vinci, M.L. Antonelli, "Biogenic amines: quality index of freshness in red and white meat", *Food Control,* vol. 13, No. 8, pp. 519-524, 2002

[3] D. Ercolini, A. Casaburi, A. Nasi, I. Ferrocino, R. Di Monaco, P. Ferranti, "Different molecular types of Pseudomonas fragi have the same overall behaviour as meat spoilers", *International Journal of Food Microbiology*, vol. 142, No. 1-2, pp. 120-131, 2010

[4] G.M. Bota, P.B. Harrington, "Direct detection of trimethylamine in meat food products using ion mobility spectrometry", *Talanta*, vol. 68, No. 3, pp. 629-635, 2006

[5] Balasubramanian, S., Panigrahi, S., Logue, C.M., Gu, H., Marchello, M., "Neural networks-integrated metal oxide-based artificial olfactory system for meat spoilage identification", *J. Food Eng.*, vol. 91, pp. 91-98, 2009

[6] Mouwen D.J.M., Hörman A., Korkeala H., Alvarez-Ordóñez A. Prieto, M., "Applying Fourier-transform infrared spectroscopy and chemometrics to the characterization and identification of lactic acid bacteria", *Vibrational Spectroscopy*, vol. 56, No. 2, pp. 193-201, 2011

[7] Wang, Q., Lonergan, S.M., Yu, C., "Rapid determination of pork sensory quality using Raman spectroscopy", *Meat Science*, vol. 91, No. 3, pp. 232-239, 2012

[8] Olsen EF, Rukke EO, Egelandsdal B, Isaksson T., "Determination of omega-6 and omega-3 fatty acids in pork adipose tissue with non-destructive Raman and Fourier transform infrared spectroscopy", *Applied Spectroscopy*, vol. 62, No. 9, pp. 968-974, 2008

[9] Kirschner C., Ofstad R., Skarpeid H. J., Host V., & Kohler A., "Monitoring of denaturation processes in aged beef loin by Fourier transform infrared microspectroscopy", *Journal of Agricultural and Food Chemistry*, vol. 52, No. 12, pp. 3920–3929, 2004

[10] Wu Z., Bertram H. C., Kohler A., Bocker U., Ofstad R. and Andersen H. J., "Influence of aging and salting on protein secondary structures and water distribution in uncooked and cooked pork. A combined FT-IR microspectroscopy and H NMR study", *Journal of Agricultural and Food Chemistry*, vol. 54, pp. 8589-8597, 2006

[11] R.R. Gangidi, A. Proctor, F.W. Pohlman, "Rapid Determination of Spinal Cord Content in Ground Beef by Attenuated Total Reflectance Fourier Transform Infrared Spectroscopy", *Journal of Food Science*, vol. 68, No, 1, pp. 124-127, 2003

[12] D.I. Ellis, D. Broadhurst, D.B. Kell, J.J. Rowland, R. Goodacre, "Rapid and quantitative detection of the microbial spoilage of meat by Fourier transform infrared spectroscopy and machine learning", *Appl. Environ. Microbiol*, vol. 68, pp. 2822–2828, 2002

[13] Argyri, A. A., Panagou, E. Z., Tarantilis, P. A., Polysiou, M., & Nychas, G.-J. E., "Rapid qualitative and quantitative detection of beef fillets spoilage based on Fourier transform infrared spectroscopy data and artificial neural networks", *Sensors and Actuators B*, vol. 145, pp. 146-154, 2010

[14] C. Bishop, *Pattern Recognition and Machine Learning*, Springer, 2007

[15] Brereton, R. G. *Applied Chemometrics for Scientists*, Wiley, 2007

[16] SYMBIOSIS-EU project, Appendix 1, 2009. Available: http://www.aua.gr/tmhmata/biomhxan/nychas/SYMBIOSIS12m/SYMBIOSIS 1stYSubRv070110 Appendix1.pdf

[17] J. Baranyi, T.A. Roberts, "A dynamic approach to predicting bacterial growth in food", *Int. J. Food Microbiol.*, vol. 23, pp. 277–294, 1994

[18] E. Wadge, V.S. Kodogiannis, D. Tomtsis, "Neuro-Fuzzy Ellipsoid Basis Function multiple classifier for diagnosis of urinary Tract Infections" *ICCMSE 2003*, Kastoria, Greece pp. 673-677, 2003

[19] L. Xu, "RBF Nets, Mixture Experts, and Bayesian Ying-Yang Learning", *Neurocomputing*, vol. 19, No. 1-3, pp. 223-257, 1998

[20] V.S. Kodogiannis, J. Lygouras, A., Tarczynski, H.S. Chowdrey, "Artificial odour discrimination system using electronic nose and neural networks for the identification of urinary track infection", *IEEE Trans. on Information Technology in Biomedicine*, vol. 12, No. 6, pp. 707-713, 2008

[21] E. Wadge, *The use of EM-Based neural network schemes for modelling and classification*, PhD Thesis, Westminster University, 2005

[22] V.S. Kodogiannis, "Decision Support Systems in Wireless-Capsule Endoscopy: Revisited", *International Journal of Intelligent Decision Technologies*, Vol. 1, No. 1,2, pp. 17-32, 2007

[23] N. Ueda, R. Nakano, "EM algorithm with split and merge operations for mixture models", *IEIC Trans. Inf. & Syst.*, Vol. 83, No. 12, pp. 2047-2055, 2000

[24] C. Sârbu, K. Zehl, and J.W. Einax, "Fuzzy divisive hierarchical clustering of soil data using Gustafson-Kessel algorithm", *Chemometrics and intelligent laboratory systems*, vol. 86, pp. 121-129, 2007

[25] V.S. Kodogiannis, I. Petrounias and J.N. Lygouras, "Intelligent Classification using Adaptive Fuzzy Logic Systems", *IS2008 – IEEE International Conference on Intelligent Systems*, pp. 8-13, 2008

[26] E.Z. Panagou, V. Kodogiannis, "Application of Neural Networks as a Non-linear Modelling Technique in Food Mycology", *Expert Systems with Applications*, vol. 36, pp. 121-131, 2009

[27] M. Amina, E.Z. Panagou, V.S. Kodogiannis and G.-J.E. Nychas, "Wavelet Neural Networks for modelling high pressure inactivation kinetics of Listeria monocytogenes in UHT whole milk", *Chemometrics and intelligent laboratory systems*, vol. 103, No. 2, pp. 170-183, 2010